Research Square

Preprints are preliminary reports that have not undergone peer review.
They should not be considered conclusive, used to inform clinical practice,
or referenced by the media as validated information.

Development of a Surgically Operable Dual-Hit Obese Rat Model of Severe Nephrotic Renal Dysfunction for Bariatric Surgery and Kidney Transplantation Research

Thibaud Bertrand
Hôpital Bichat-Claude-Bernard
Tigran Poghosyan
tigran.poghosyan@aphp.fr
Hôpital Bichat-Claude-Bernard
Alexandra Willemetz
Centre de Recherche sur l'Inflammation
Edouard Guenzi
Hôpital Bichat-Claude-Bernard
Marc-Anthony Chouillard
Hôpital Bichat-Claude-Bernard
Aurélie Sannier
Hôpital Bichat-Claude-Bernard
André Bado
Centre de Recherche sur l'Inflammation
Maude le Gall
Centre de Recherche sur l'Inflammation
Lara Ribeiro-Parenti
Hôpital Bichat-Claude-Bernard

Research Article

Keywords: Obesity-related glomerulopathy, Adriamycin nephropathy, Severe nephrotic renal dysfunction, Bariatric surgery, Sleeve gastrectomy, Kidney transplantation, Rat model.

Posted Date: November 12th, 2026

DOI: https://doi.org/10.21203/rs.3.rs-11295377/v1

License: This work is licensed under a Creative Commons Attribution 4.0 International License.
Read Full License

Additional Declarations: No competing interests reported.

Development of a Surgically Operable Dual-Hit Obese Rat Model of Severe Nephrotic Renal Dysfunction for Bariatric Surgery and Kidney Transplantation Research

Abstract

Introduction :
Severe obesity-related glomerulopathy (ORG) progressing to end-stage renal disease (ESRD) represents a growing challenge in kidney transplantation. Metabolic bariatric surgery (MBS) is increasingly proposed as a "bridge" to transplantation, yet no preclinical model reproduces the clinical triad of advanced obesity, nephrotic renal failure, and surgical operability. We aimed to develop and characterize a dual-hit obese rat model of severe nephrotic renal dysfunction approaching end-stage renal disease (ESRD), compatible with bariatric surgery and orthotopic kidney transplantation (KT).

Methods :
Male Wistar rats were fed a high-fat diet for 16 weeks to induce obesity, followed by titrated transjugular adriamycin (ADR) injection (3–9 mg/kg) to induce nephropathy. Renal function (estimated creatinine clearance), nephrotic parameters (proteinuria, albumin, triglycerides), and histological injury were assessed. Surgical feasibility of sleeve gastrectomy (SG), Roux-en-Y gastric bypass (RYGB), and orthotopic KT was evaluated. Analyses were descriptive due to the exploratory design.

Results :
Transjugular ADR provided reproducible renal injury with reduced local complications compared to caudal injection. High doses (6–9 mg/kg) induced excessive early mortality. ADR 3–4 mg/kg established a severe nephrotic phenotype while preserving short-term survival, defining a surgical window. RYGB was associated with 100% early postoperative mortality (0/6) in these rats. In contrast, SG was feasible, with approximately half of operated animals surviving over 10 days (9/17). Histology demonstrated dose-dependent tubulointerstitial injury; after SG, inflammatory and acute tubular lesion scores were descriptively lower, although the small subgroup sizes preclude any efficacy interpretation. Orthotopic KT was technically achievable despite increased visceral adiposity, although long-term survival remained limited.

Conclusion:
We developed a reproducible dual-hit obese rat model of severe nephrotic renal dysfunction approaching ESRD that preserves surgical operability. These exploratory findings are hypothesis-generating and provide a platform to investigate metabolic bridge strategies and graft behavior in high-risk recipients with obesity and advanced renal disease.

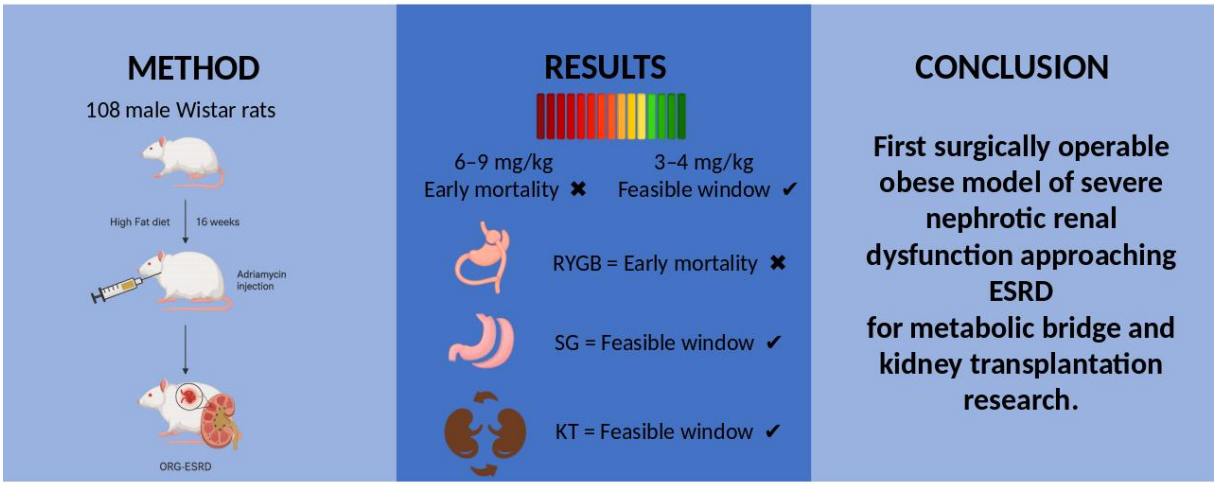
Key Points

- We developed a reproducible dual-hit rat model combining diet-induced obesity and adriamycin-induced nephropathy progressing toward severe nephrotic renal dysfunction approaching ESRD while preserving surgical operability.
- A narrow 3-4 mg/kg adriamycin window balanced severe nephrotic renal dysfunction with short-term survival, defining a surgical window.
- Sleeve gastrectomy was feasible in ORG-ESRD rats, whereas Roux-en-Y gastric bypass was associated with prohibitive early mortality.
- This platform enables translational investigation of metabolic bridge strategies and kidney transplantation in high-risk recipients with obesity and advanced renal disease.

Key Words : **Obesity-related glomerulopathy; Adriamycin nephropathy; Severe nephrotic renal dysfunction; Bariatric surgery; Sleeve gastrectomy; Kidney transplantation; Rat model.**

Graphical Abstract

Dual-Hit Obese Rat Model of Severe Nephrotic Renal Dysfunction for Bariatric Surgery and Kidney Transplantation



IFSO

(Please keep this space clear for review purposes)

OBESITY SURGERY
The Journal of Metabolic Surgery and Allied Care

Introduction

Obesity has emerged as a systemic disease and a global epidemic, becoming a primary driver of chronic kidney disease (CKD) [1,2]. Obesity-related glomerulopathy (ORG) is a well-defined entity characterized pathologically by glomerulomegaly and adaptive focal segmental glomerulosclerosis (FSGS) [3–5]. Clinically, ORG manifests as progressive proteinuria and an insidious decline in the glomerular filtration rate (GFR); in approximately 10% to 33% of cases, it advances to end-stage renal disease (ESRD) requiring renal replacement therapy [6–8].

While kidney transplantation (KT) remains the treatment of choice for ESRD, individuals with severe obesity face significant barriers to access [9,10]. Obesity is associated with increased perioperative risks, delayed graft function, and impaired long-term outcomes [11,12]. To mitigate these risks and improve eligibility, current clinical guidelines—including the KDIGO 2020 guideline on the evaluation of kidney transplant candidates and the ERA DESCARTES recommendations on the management of obesity in transplant candidates, as well as the Association Française d'Urologie 2025 recommendations—increasingly advocate for a "metabolic bridge" using metabolic bariatric surgery (MBS) prior to KT, in line with the 2022 ASMBS/IFSO indications [13–17]. Consequently, transplant surgeons frequently manage candidates under highly inflammatory and nephrotic conditions where surgical complexity is compounded by increased visceral adiposity [18].

Despite the proliferation of preclinical models for kidney disease, few successfully reproduce this specific clinical triad: severe obesity, nephrotic-range renal failure, and surgical operability [19]. Adriamycin (ADR)-induced nephropathy is the established rodent model for FSGS and nephrotic syndrome, but its high systemic toxicity often results in narrow survival windows [20–23]. Traditional administration via the caudal vein frequently leads to local necrosis and unpredictable bioavailability, which limits the use of these animals as a stable platform for complex abdominal surgery [24–26].

Throughout this report, “ORG-ESRD” denotes the achieved obese, severe nephrotic phenotype approaching end-stage renal disease and is used as an operational label, given that renal function was estimated rather than directly measured. To address this gap, the present study aimed to develop and characterize a "dual-hit" ORG-ESRD rat model optimized for complex surgery. The rat was selected over smaller rodent models due to its well-documented suitability for operating microscopy and reproducible vascular and digestive suturing [27,28]. We used male Wistar rats, as they exhibit a reliable response to diet-induced obesity (HFD), developing hyperlipidemia, insulin resistance, and increased visceral fat that mimics human pathology. By combining 16 weeks of HFD with a titrated, transjugular injection of ADR, we sought to induce a reproducible state of terminal renal failure—defined as ≤30% residual function associated with a complete nephrotic syndrome—while preserving sufficient survival for surgical intervention. It should be emphasized that adriamycin nephropathy is a toxic, predominantly acute model of direct podocyte injury and does not reproduce the spontaneous, hyperfiltration-driven chronic course of human obesity-related glomerulopathy; here it is used to generate, in a controlled and reproducible timeframe, a nephrotic FSGS-like phenotype compatible with complex abdominal and vascular surgery.

Rather than focusing on therapeutic efficacy, the overarching objective was to establish a robust and surgically accessible experimental platform. The central research question was whether a reproducible obese rat model combining advanced renal dysfunction and nephrotic syndrome could be developed while remaining compatible with complex surgical procedures. The primary objective was therefore to create and characterize an ORG model progressing toward ESRD that preserves surgical operability. Secondary objectives included optimization of ADR dose and administration route to balance disease severity with survival, phenotypic characterization of renal and metabolic alterations, and assessment of the technical feasibility of MBS and orthotopic KT in this setting.

The study was based on the working hypotheses that (i) combining diet-induced obesity with ADR-induced nephropathy would generate a severe renal phenotype mimicking advanced ORG, (ii) dose titration would identify a window reconciling renal severity with surgical feasibility, and (iii) complex microsurgical procedures would remain technically achievable despite increased visceral adiposity and nephrotic status. Such a platform is essential for simulating high-risk clinical scenarios encountered in patients with obesity awaiting transplantation and for investigating graft behavior in a metabolically hostile post-bariatric host.

Methods

Animals

Male Wistar rats aged 6 weeks and weighing between 220 and 240 g at arrival were used in this study. Rats were obtained from an approved commercial breeder and were specific pathogen-free (SPF) at the time of arrival. Animals were not genetically modified and were clinically healthy at the start of experimental procedures. Only male animals were included to avoid potential variability related to hormonal cycling. Animals were housed by six in ventilated transparent plastic cages (IVC system) within a SPF facility. Environmental enrichment consisted of nesting cotton material and a plastic shelter within each cage to allow hiding behavior and promote welfare. Animals were acclimatized for at least 7 days before any procedure. Prior to surgical procedures, rats were group-housed (three animals per cage) with standard bedding material to promote social interaction.

The animal room was maintained at a controlled temperature of 21–23°C with relative humidity of 45–65% and a 12-hour light/dark cycle. Food and water were provided ad libitum throughout the study, except during preoperative fasting periods.

To induce obesity, rats were fed a high-fat diet (HFD; Altromin C45, Genestil, Royaucourt, France) for a duration of 3 months prior to ADR administration. After this period, obese animals typically exceeded 500 g in body weight and were used for ORG-ESRD model development and subsequent surgical procedures. Lean control male Wistar rats used for technical ADR injection and kidney transplantation development were maintained on a standard laboratory diet throughout the study.

Following surgical procedures, animals were housed individually for 15 days to allow close postoperative monitoring, prevent wound interference by cage mates, and facilitate precise fluid and feeding management.

All surgical procedures were performed in the dedicated rodent operating room under inhalational anesthesia using isoflurane delivered via an anesthesia machine equipped with charcoal filters, according to the laboratory operating procedure. Anesthesia induction was performed with 5% isoflurane in oxygen, followed by maintenance with inhaled isoflurane adjusted to surgical depth (recorded individually in operative sheets). Animals were placed on heated pads to maintain normothermia.

Perioperative fluid support was systematically administered to minimize renal hypoperfusion and dehydration. A structured postoperative refeeding protocol was implemented. Predefined humane endpoints were established prior to study initiation. Animals were monitored daily using a structured clinical scoring system ranging from 0 to 38 (Supplementary material 1).

Immediate euthanasia was performed in cases of: ≥30% body weight loss, immobility or inability to access food or water,

Clinical score ≥15 (predefined humane limit point). Postoperative analgesia was provided as needed. Euthanasia was performed using isoflurane overdose.

Expected adverse events included weight loss, proteinuria, hypoalbuminaemia, and hypertriglyceridaemia related to ADR-induced nephropathy.

Surgical adverse events observed during the study included anastomotic fistula, sleeve leak, aspiration, anaesthetic complications, and early postoperative mortality. In the high-dose ADR groups (6 and 9 mg/kg), severe early mortality occurred due to excessive systemic toxicity.

No unexpected adverse events outside the anticipated renal and surgical complications were observed.

Study design and experimental groups

This work comprised successive experimental series aimed at developing and validating: (i) a transjugular adriamycin (ADR) injection technique, (ii) an ORG-ESRD rat model using varying

ADR doses and different timings of bariatric surgery after ADR injection, and (iii) the surgical feasibility of kidney transplantation in ORG-ESRD context.

Given the iterative nature of model and technique development, no single a priori comparative design with fixed parallel groups was implemented. The rationale was that the study was designed for incremental validation of surgical feasibility and dose/timing titration, making traditional controls for every sub-step ethically redundant. Unblinded allocation to experimental series and subgroups was performed sequentially according to the iterative requirements of model development, dose titration, and surgical feasibility assessment. To minimise systematic bias, all animals were housed under identical environmental conditions (temperature, light–dark cycle, and diet), and surgical and laboratory procedures were standardised across experimental series. Biological measurements were performed using the same analytical methods throughout the study period.

Importantly, the surgical learning curve for bariatric procedures (Roux-en-Y gastric bypass and sleeve gastrectomy) had been completed in separate laboratory projects prior to the present study. A stable technical performance was achieved, defined by a 15-day postoperative survival rate of approximately 15% for RYGB and 0% for SG. Therefore, surgical outcomes in this study were not influenced by early-phase operator learning effects.

Experimental series included: (1) technical development of ADR injection in lean rats (n=16); (2) development and optimization of an ORG-ESRD model in obese rats with exploratory bariatric surgery attempts (n=47 ; RYGB : 6 ; SG : 17); (3) autotransplantation feasibility (n=10); and (4–5) kidney transplantation feasibility and attempts in ORG-ESRD recipients (n=13 recipients and 13 donors ; n= 9 donors and 9 animals from Series 2). Overall, the total number of animals used in this study was 108, including 22 donor animals (13 in Series 4 and 9 in Series 5).

The experimental unit was a single animal. Donor animals were reported as part of total animal use but were not considered experimental units for recipient outcome analyses.

Inclusion criteria comprised all animals undergoing the planned experimental procedures. Criteria were established a priori. For analyses intended to evaluate the effect of bariatric surgery on the ORG-ESRD model, animals were required to survive at least 10 days after bariatric surgery to be considered eligible for outcome assessment (Figure 1).

Animals that did not meet this survival threshold were not excluded from the experimental series and were retained for reporting of ADR exposure, surgical feasibility, and early postoperative mortality. No data points were excluded on the basis of outcome values.

Definition of outcomes

Outcome assessment was performed under blind conditions. The biochemist responsible for laboratory measurements and the pathologist performing histological evaluation were unaware of the treatment allocation of the animals. Samples and histological slides were coded prior to analysis to ensure assessor blinding.

Outcome measures were defined according to the objective of each experimental series.

(i) Feasibility outcomes included perioperative survival, early postoperative mortality (<10 days), and procedure-related complications (e.g., fistula, aspiration, anaesthetic complications).

(ii) Renal functional outcomes included estimated creatinine clearance calculated using the ACLARA equation (to approximate GFR) when available [29]. When body weight exceeded 700 g, it was truncated at 700 g for the purpose of estimation to avoid extrapolation beyond the validated range of the equation.

(iii) Nephrotic syndrome–related outcomes included proteinuria (>30 g/L), albuminemia (<30 g/L), and triglyceride levels (mmol/L), reflecting glomerular injury severity.

(iv) Body weight evolution was analysed separately to assess the metabolic effect of bariatric surgery.

(v) Histological outcomes consisted of renal structural assessment derived from semi-quantitative histological grading performed on haematoxylin–eosin and additional staining when available, evaluating glomerular and tubulointerstitial lesions consistent with ORG-ESRD [21,30].

For analyses evaluating the effect of bariatric surgery on the ORG-ESRD model, the co-primary outcomes for these analyses were:

(i) renal function, assessed by estimated creatinine clearance (ACLARA equation), and

(ii) renal histological injury severity.

Secondary outcomes included urinary protein excretion, albumin concentration, triglyceride levels, perioperative survival.

Procedures

Adriamycin (ADR) was administered via intravenous injection using either a transjugular or caudal vein approach, depending on the experimental series under general anesthesia. Different doses (3, 4, 6, or 9 mg/kg) were evaluated during model optimisation. The transjugular approach was developed to improve reproducibility of systemic delivery.

Bariatric surgery was performed under general anaesthesia using standard surgical techniques. Procedures included sleeve gastrectomy (SG) or Roux-en-Y gastric bypass (RYGB), depending on the subgroup. They were previously described [28,31]. Sleeve gastrectomy (SG) consisted of removal of the forestomach and resection of approximately 80% of the gastric fundus using a 35-mm ETS-Flex stapler, resulting in the creation of a tubular gastric remnant. Roux-en-Y gastric bypass (RYGB) involved the construction of a 20% gastric pouch using a TX30V stapler, jejunal transection 20 cm distal to the pylorus, creation of a gastrojejunal anastomosis, and a jejunojejunal anastomosis performed 15 cm distally using 7-0 Prolene sutures. Sham

surgery consisted of gastric and jejunal manipulation without resection, followed by abdominal wall closure with 4-0 and 3-0 Vicryl sutures. Surgery was performed either 2 or 4 weeks after ADR injection, according to the experimental protocol.

Renal autotransplantation procedures were performed to establish microsurgical feasibility of vascular anastomosis techniques prior to allogeneic transplantation. Orthotopic KT was performed using standard microsurgical techniques with vascular anastomosis of the renal artery and vein. Donor nephrectomy and recipient implantation were performed under general anaesthesia (Figure 2).

Blood (via tail vein or saphenous puncture) and urine samples were collected at predefined time points throughout follow-up. At experimental endpoints or humane criteria, animals were euthanised (isoflurane overdose). Both kidneys were harvested, fixed overnight in 10% neutral buffered formalin, paraffin-embedded, sectioned at 4 µm, and stained with: HES/PAS/Perls/Masson trichrome. Renal histological injury was assessed semi-quantitatively by a single pathologist blinded to group allocation. For each animal, 50 glomeruli and 30 grid fields of the renal cortex (0.1 mm^2 each) were examined at ×400 magnification, following the standardized approach validated in adriamycin nephropathy by Faleiros et al. [20]. Four compartments were graded on a 0–3 ordinal scale (0 = absent/normal; 1 = mild, <25%; 2 = moderate, 25–50%; 3 = severe, >50% of the assessed area): interstitial inflammation, interstitial fibrosis, tubular atrophy, and acute tubular necrosis. Glomerular changes (glomerulomegaly, segmental sclerosis) were scored on the same 50 glomeruli, and criteria were defined a priori and applied uniformly across series.

Statistical Analyses

Statistical analyses were performed using GraphPad Prism version 9 (GraphPad Software, San Diego, CA, USA).

Continuous variables are presented as median [range] when appropriate.

Given the exploratory nature of the study and the small, uneven subgroup sizes, only descriptive analyses were performed. No inferential statistical tests were applied, and no confidence intervals or effect-size estimates were computed; all between-group differences are reported descriptively (median [range]) and should be regarded as hypothesis-generating only. No formal a priori sample-size calculation was performed: animal numbers reflect the iterative requirements of technique development and dose titration and the 3Rs principle of minimizing animal use and were not powered for hypothesis testing.

(i) Series 1 (ADR injection technique development, lean rats; n = 16): all animals were included in the analysis.

(ii) Series 2 (ORG-ESRD model development, obese rats; n = 47): all animals were included in the reporting of experimental allocation and model development. Subgroups reflected exploratory optimization steps rather than predefined comparative groups.

For analyses evaluating the effect of bariatric surgery on the ORG-ESRD model :

RYGB: no animals met eligibility criteria for bariatric effect analysis (0 included), due to early postoperative mortality.

- ADR 4 mg groups:

ADR 4 mg alone: 7 animals were eligible for analysis. Five subsequently underwent kidney transplantation, the last available blood and urine samples collected on the day of transplantation were used for functional analysis. Histological evaluation was performed on the explanted native kidney obtained at the time of nephrectomy. This approach ensured that renal functional and structural assessments reflected the pre-transplant disease status at the time of surgical intervention. Exclusions from bariatric effect analysis were due to: respiratory failure after ADR injection (n = 1), RYGB fistula (n = 3), RYGB humane endpoint reached (n = 1),

aspiration after RYGB (n = 1), anesthetic overdose during RYGB (n = 1), missing histology (n = 2), SG humane endpoint (n = 1), and SG fistula (n = 2).

ADR 4 mg + SG at 4 weeks: 3 animals included.

ADR 4 mg + SG at 2 weeks: 2 animals included. They subsequently underwent kidney transplantation, the last available blood and urine samples collected on the day of transplantation were used for functional analysis. Histological evaluation was performed on the explanted native kidney obtained at the time of nephrectomy. This approach ensured that renal functional and structural assessments reflected the pre-transplant disease status at the time of surgical intervention.

- ADR 3 mg groups:

ADR 3 mg alone: 3 animals eligible. Two subsequently underwent kidney transplantation, the last available blood and urine samples collected on the day of transplantation were used for functional analysis. Histological evaluation was performed on the explanted native kidney obtained at the time of nephrectomy. This approach ensured that renal functional and structural assessments reflected the pre-transplant disease status at the time of surgical intervention. Exclusions for bariatric analysis were due to air embolism during ADR injection (n = 1) and SG humane endpoints reached (n = 2).

ADR 3 mg + SG at 2 weeks: 4 animals included; exclusions were due to sleeve fistula (n=3).

Saline + sham at 2 weeks: 3 animals included.

(iii) Series 3 (autotransplantation feasibility; n = 10): all animals included.

(iv) Series 4 (kidney transplantation feasibility; recipients n = 13, donors n = 13): only recipients included.

(v) Series 5 (kidney transplantation attempts in ORG-ESRD rats; donors n = 9): only recipient included; recipient animals are reported within Series 2. The two

transplanted animals that had previously undergone sleeve gastrectomy were excluded to ensure model uniformity.

Results

Series 1 – Optimization of ADR administration and model definition

In lean rats (n = 16), renal function was first assessed at baseline. Rats received intravenous ADR and were re-evaluated 4 weeks later using identical biological and imaging assessments. End-stage renal disease (ESRD) was defined as ≤30% residual renal function compared to baseline, associated with a nephrotic syndrome.

Three injection approaches were assessed: an initial caudal vein injection (6 mg/kg, solvent- or saline-diluted, with solvent controls), a Veinlite-assisted optimized caudal protocol using 6–12 mg/kg ADR in solvent, and a transjugular approach implemented after excessive mortality related to caudal extravasation. Renal impairment occurred exclusively in rats receiving ADR diluted in the manufacturer's solvent. ADR diluted in saline failed to induce significant renal dysfunction, indicating insufficient bioavailability. The solvent alone had no detectable renal effect.

At 4 weeks, residual creatinine clearance was approximately 47% following caudal injection of 6 mg/kg ADR (solvent-based), compared with ~30% after jugular injection of 6 mg/kg and ~25% after jugular injection of 9 mg/kg. A complete nephrotic syndrome (albumin <30 g/L, proteinuria >30 g/L, hypertriglyceridemia) was observed only in ADR/solvent groups. Other urinary indices were not discriminant (Supplementary material 2).

Given improved reproducibility and reduced extravasation-related mortality, the transjugular route was retained for subsequent experimental series.

Series 2 – Development and optimization of the obese ORG-ESRD model

Forty-seven obese rats were included in model optimization experiments. ADR doses of 9, 6, 4, and 3 mg/kg were evaluated in combination with variable timing of bariatric surgery.

ADR 9 and 6 mg/kg were associated with marked early mortality and severe renal impairment, limiting longitudinal evaluation (median overall survival after injection 0 days (0-7) and 7,5

days (7-8)). ADR 4 and 3mg/kg provided sustained survival (median overall survival after injection 34 days (6-62) and 25 days (0-50) (Table 1 ; Figure 3).

ADR 4 mg/kg induced rapid and pronounced renal dysfunction with high early postoperative vulnerability. In contrast, ADR 3 mg/kg induced sustained renal injury while preserving short-term survival, allowing assessment of surgical intervention. RYGB was attempted in six obese ORG-ESRD rats but was associated with 100% early postoperative mortality, primarily due to anastomotic complications and clinical deterioration. In contrast, SG demonstrated improved short-term feasibility, with 9 of 17 animals surviving beyond 10 postoperative days and being eligible for renal outcome analysis. The main SG-related complication was SG fistula. (Table 2; Figure 1 ; Figure 4).

Histological lesions were dose-dependent, with more severe changes observed in the 4 mg/kg group compared to the 3 mg/kg group. In the bariatric-effect series, compared with lean PHy + SHAM controls (score 0–1 across parameters), ORG-ESRD rats developed marked dose-dependent tubulointerstitial injury characterized by inflammatory infiltrates, interstitial fibrosis, tubular atrophy, and acute tubular necrosis (ATN). After SG, descriptively lower fibrosis, tubular atrophy and ATN scores were observed; given the small subgroup sizes, these differences are hypothesis-generating only and are not interpreted as a protective effect (Supplementary material 3).

Table 1 : Renal and metabolic parameters at the latest available time point in Series 2

Group	n	Early mortality (before 10 days after ADR)	n analysed	Median follow-up days after ADR	Creatinine clearance (mL/min)	Albumin (g/L)	Proteinuria (g/L)	Triglycerides (mmol/L)	Weight Loss (g)
ADR 9 mg/kg	5	5	0	0 (0-7)	Not applicable (no surviving animals for analysis)				
ADR 6 mg/kg	2	2	0	7.5 (7-8)					
ADR 4mg/kg	19	1	18	32 (17-49)	0.87 (0.2-2.8)	20.5 (8.3-35.3)	51.3 (0,3-163.5)	7.2 (1.73-20.3)	108 (3-217)
ADR 4mg/kg + SG4w	3	0	3	51 (37-62)	1.27 (0.6-2.1)	19 (16.2-23.5)	66.5 (58.3-237)	12.8 (12.1-17.6)	280 (234-322)
ADR 4mg/kg + SG2w	2	0	2	34 (27-41)	0.18 (0.1-0.3)	18.6 (17.5-19.6)	58.8 (49.5-68)	3.9 (3.6-4.2)	195 (176-213)
ADR 3mg/kg	6	1	3	38 (16-50)	0.98 (0.7-2.7)	19 (18.9-20.2)	43.5 (39.5-45)	27 (18.4-28.4)	117 (85-135)
ADR 3mg/kg + SG2w	7	0	7	25 (24-27)	0.89 (0.8-1.5)	17.9 (15.1-19.6)	63 (37-97.5)	4.2 (1.2-13.8)	127 (70-144)
Phy + SHAM	3	0	3	29 (29-29)	2 (1.5-2.2)	19.6 (19.4-21.6)	59.5 (36.5-91.5)	11.5 (7.3-18.5)	68 (6-124)

Continuous variables are presented as median [range] due to small sample sizes and non-normal distribution.

Data are shown as median (range).

Table 2 : Renal and metabolic parameters at the latest available time point in bariatric surgical procedures

Group	n analysed	Median follow-up days after ADR	Median follow-up days after BS	Creatinine clearance (mL/min)	Albumin (g/L)	Proteinuria (g/L)	Triglycerides (mmol/L)	Weight Loss (g)
ADR 4mg/kg	7	41 (24-49)	NA	0.58 (0.19-2.8)	22.2 (8.3-35.3)	35.3 (34.5-36)*	2.76 (1.73-10.2)	110 (84-175)
ADR 4mg/kg + SG4w	3	51 (37-62)	21 (10-32)	1.27 (0.44-2.1)	19 (16.2-23.5)	66.5 (58.3-237)	12.8 (12.1-17.6)	280 (234-322)
ADR 4mg/kg + SG2w	2	34 (27-41)	18.5 (13-24)	0.18 (0.09-0.27)	18.55 (17.5-19.6)	58.8 (49.5-68)	3.9 (3.6-4.2)	388.5 (367-410)
ADR 3mg/kg	3	40 (38-50)	NA	1.25 (0.73-2.69)	19 (18.9-20.2)	43.5 (39.5-45)	27 (18.4-28.4)	123 (85-135)
ADR 3mg/kg + SG2w	4	24.5 (24-27)	11.5 (10-13)	0.85 (0.8-1.2)	18.3 (15.1-19.6)	63.5 (41-97.5)	3.63 (1.2-10.5)	122 (70-139)
Phy + SHAM	3	29 (29-29)	14 (14-14)	2.05 (1.52-2.18)	19.6 (19.4-21.6)	59.5 (36.5-91.5)	11.5 (7.3-18.5)	68 (6-124)

Continuous variables are presented as median [range] due to small sample sizes and non-normal distribution.

*Only 2 urine samples available

Series 3 – Autotransplantation

Autotransplantation was performed to validate microsurgical vascular anastomosis techniques prior to allogeneic transplantation. Warm ischemia time, vascular clamp time, and total operative time progressively decreased during the series, reflecting procedural standardisation. Perioperative survival was achieved in the majority of animals, confirming the technical reproducibility of renal vascular anastomosis in the rat model (Supplementary material 4).

Series 4 – Allogeneic kidney transplantation

Thirteen recipient rats underwent orthotopic kidney transplantation with corresponding donors. Early postoperative survival confirmed the feasibility of transplantation under experimental conditions. This series validated the reproducibility of the surgical protocol prior to its application in obese ORG-ESRD animals (Supplementary material 4).

Series 5 – Transplantation in ORG-ESRD rats

Kidney transplantation was subsequently attempted in obese rats with established ORG-ESRD. Nine donor animals were used. Recipient animals originated from Series 2. Surgery was technically feasible despite increased visceral adiposity and altered tissue planes. However, postoperative survival was limited, with only one recipient surviving to postoperative day 8 (Supplementary material 4, Supplementary video A1-6). Despite limited survival, vascular anastomosis and graft reperfusion were technically achievable in the ORG-ESRD context.

Discussion

The present study describes the development and characterization of a reproducible dual-hit rat model combining diet-induced obesity and adriamycin-induced nephropathy, progressing toward severe nephrotic renal dysfunction approaching ESRD, while preserving surgical operability. Three major findings emerge. First, transjugular administration of adriamycin (ADR) provides superior reproducibility and reduced local complications compared with caudal vein injection, enabling controlled induction of nephrotic renal failure [24–26]. Second, a narrow dose window between 3 and 4 mg/kg ADR reconciles severe renal impairment with short-term survival, thereby allowing the performance of complex abdominal procedures. Third, SG is technically feasible in this hostile metabolic and inflammatory environment, whereas RYGB is associated with prohibitive early postoperative mortality. Orthotopic KT remains technically achievable, although survival is limited in the most severe phenotypes. Collectively, these findings establish a surgically accessible ORG-ESRD platform that mimics high-risk transplant candidates and enables future investigation of metabolic bridge strategies.

Experimental nephropathy models have traditionally focused on isolated renal injury. The ADR model is well established as a model of FSGS and nephrotic syndrome, but it is typically applied in lean animals [21]. Conversely, HFD models reproduce obesity-associated metabolic disturbances but rarely progress to severe renal failure within practical timeframes [32,33]. Few preclinical systems combine advanced obesity, nephrotic-range proteinuria, and surgical feasibility [34]. The originality of the present work lies in the integration of these elements into a single, operable platform. By combining prolonged HFD exposure with titrated transjugular ADR injection, we reproduced a phenotype characterized by visceral adiposity, hypoalbuminemia, hypertriglyceridemia, reduced creatinine clearance, and histological lesions consistent with ORG-ESRD, including interstitial inflammation, fibrosis,

tubular atrophy, and superimposed acute tubular necrosis. Importantly, the study was not designed to demonstrate therapeutic efficacy but to define the boundaries of feasibility—renal severity sufficient to model advanced disease, yet compatible with complex microsurgery. In that respect, this model addresses a gap between nephrology-focused animal research and surgical translational studies. A mechanistic caveat warrants emphasis: although ORG and ADR nephropathy converge on a common phenotype of podocyte injury and focal segmental glomerulosclerosis, their mechanisms differ. Human ORG is driven primarily by chronic glomerular hyperfiltration and slowly progressive adaptive injury, whereas ADR nephropathy reflects relatively acute, direct toxic podocyte damage. This model should therefore be regarded as a phenotypic and operative surrogate rather than a faithful reproduction of the natural history of ORG. It is best suited to questions in which the relevant variable is the host surgical and metabolic environment — perioperative tolerance of bariatric and transplant procedures in a recipient with obesity, nephrotic syndrome, hypoalbuminaemia and systemic inflammation; graft behaviour and ischaemia–reperfusion injury in a metabolically hostile host; and the timing and impact of a metabolic bridge before transplantation. Conversely, it is less appropriate for studying the early pathogenesis or the chronic, hyperfiltration-driven progression of ORG itself, for which spontaneous, dietary or genetic obese-nephropathy models are preferable.

A central finding is the identification of a narrow therapeutic window between renal severity and survival. High doses (6–9 mg/kg) induced excessive early mortality and precluded longitudinal follow-up. In contrast, 3 and 4 mg/kg doses generated sustained renal dysfunction while maintaining a subset of animals suitable for surgical intervention. The 4 mg/kg dose induced more severe histological injury and functional decline but was associated with increased postoperative vulnerability. The 3 mg/kg dose provided a more balanced phenotype, preserving survival while maintaining clear nephrotic features. This dose-response

relationship underscores the concept of a “surgical window” in experimental ESRD models. Excessive toxicity compromises not only survival but also the interpretability of surgical outcomes. Conversely, insufficient renal injury fails to reproduce the inflammatory and metabolic hostility encountered in clinical transplant candidates. The identification of this window is therefore essential for future interventional studies.

One of the most clinically relevant observations is the differential feasibility of bariatric procedures. RYGB was associated with 100% early postoperative mortality in ORG-ESRD rats. Complications included anastomotic fistula, aspiration, and rapid clinical deterioration. This high failure rate likely reflects the combined effects of hypoalbuminemia, systemic inflammation, and impaired wound healing in nephrotic animals. The catabolic state induced by ADR nephropathy may exacerbate anastomotic fragility and increase susceptibility to sepsis. In contrast, SG demonstrated improved short-term feasibility. Approximately half of SG-operated animals survived beyond 10 postoperative days and were eligible for renal outcome assessment. Although complications such as sleeve fistula occurred, the overall procedural tolerance was markedly superior to RYGB. From a translational perspective, this differential tolerance is highly informative [35]. It suggests that restrictive procedures may be better suited than bypass procedures in severely nephrotic, inflamed hosts—at least in the short term. While extrapolation to humans must be cautious, the model provides a mechanistic framework to investigate how hypoalbuminemia and systemic inflammation influence surgical healing.

Histological analysis confirmed dose-dependent tubulointerstitial injury, with more severe inflammatory infiltrates, fibrosis, and tubular atrophy in the 4 mg/kg group. ATN appeared particularly sensitive to bariatric intervention, whereas chronic lesions such as fibrosis and atrophy showed only partial attenuation. Because the exploratory design and small subgroup sizes precluded inferential statistical testing, these observations are descriptive and

hypothesis-generating only; they suggest, without demonstrating, that SG might be associated with lower inflammatory activity and acute tubular injury. This apparent pattern must also be interpreted in the light of survivorship bias. These findings are consistent with known anti-inflammatory and metabolic effects of bariatric surgery [34]. Importantly, functional and structural assessments were synchronized with the timing of transplantation when applicable, ensuring that measurements reflected the disease state at surgical intervention. This strengthens the translational relevance of the data.

The transplantation series demonstrate that vascular anastomosis and graft reperfusion are technically achievable in ORG-ESRD rats. Increased visceral adiposity, altered tissue planes, and fragile vessels complicate exposure and prolong operative time [36]. Nevertheless, procedural standardization and learning-curve optimization enabled reproducible vascular reconstruction [37]. Postoperative survival remained limited in the most severe phenotypes. Early deaths were attributable to anesthesia intolerance, vascular complications, or systemic deterioration rather than technical impossibility. The observation that graft reperfusion and early function can be achieved in this context confirms that the platform is surgically viable, even if long-term survival remains to be optimized. This finding is crucial for future studies evaluating graft behavior in metabolically compromised recipients or investigating the impact of pre-transplant metabolic interventions.

Several limitations must be acknowledged. First, the study followed an iterative, feasibility-driven design without formal randomization or inferential statistical comparisons. Subgroup sizes were small, reflecting the exploratory objective.

Second, the analyses of the effect of bariatric surgery are subject to survivorship bias, as only animals surviving beyond the predefined 10-day postoperative threshold were eligible for renal functional and histological assessment; the descriptively more favourable profile after SG may therefore partly reflect selective survival of less severely injured animals rather than

a genuine protective effect. Third, renal function was estimated using the ACLARA equation rather than measured by clearance or GFR, so the degree of renal failure is approximated; we therefore describe the phenotype as severe nephrotic renal dysfunction approaching ESRD. Fourth, only male rats were included, limiting generalizability across sexes. Fifth, postoperative survival after transplantation in the most severely affected animals was limited, restricting long-term graft evaluation. Finally, the model reflects acute toxic nephropathy superimposed on diet-induced obesity and, as discussed above, does not reproduce the chronic, hyperfiltration-driven course of human ORG. Despite these limitations, the study achieves its primary objective: defining a reproducible and surgically operable platform. Patients with severe obesity and ESRD represent a growing clinical challenge [38]. They frequently present with systemic inflammation, nephrotic syndrome, and impaired healing—factors that complicate both bariatric surgery and transplantation. The present model reproduces key elements of this high-risk phenotype. By establishing a platform compatible with both metabolic surgery and kidney transplantation, this work enables future mechanistic studies addressing: the optimal timing of bariatric intervention before transplantation; the impact of weight loss on graft susceptibility to ischemia-reperfusion injury; the influence of metabolic improvement on post-transplant outcomes.

Rather than demonstrating efficacy, the present study lays the groundwork for hypothesis-driven interventional trials in a controlled experimental setting.

Conclusion

We developed a reproducible dual-hit obese rat model of severe nephrotic renal dysfunction approaching ESRD that preserves surgical operability. A transjugular ADR approach and dose titration identified a narrow window balancing renal severity and survival. Sleeve gastrectomy is feasible in this context, whereas Roux-en-Y gastric bypass is poorly tolerated.

Orthotopic kidney transplantation remains technically achievable despite increased visceral adiposity and nephrotic status.

This model provides a unique translational platform for investigating metabolic bridge strategies and graft behavior in high-risk recipients with obesity and advanced renal disease.

References

[1] Nawaz S, Chinnadurai R, Al-Chalabi S, Evans P, Kalra PA, Syed AA, et al. Obesity and chronic kidney disease: A current review. Obes Sci Pract 2023;9:61–74. https://doi.org/10.1002/osp4.629.

[2] Rico-Fontalvo J, Ciudin A, Correa-Rotter R, Díaz-Crespo FJ, Bonanno C, Lecube A, et al. S.E.N., SLANH, and SEEDO consensus report on obesity-related kidney disease: proposal for a new classification. Kidney Int 2025;108:572–83. https://doi.org/10.1016/j.kint.2025.06.013.

[3] Darouich S, Goucha R, Jaafoura MH, Zekri S, Ben Maiz H, Kheder A. Clinicopathological characteristics of obesity-associated focal segmental glomerulosclerosis. Ultrastruct Pathol 2011;35:176–82. https://doi.org/10.3109/01913123.2011.584657.

[4] Tsuboi N, Okabayashi Y. The Renal Pathology of Obesity: Structure-Function Correlations. Seminars in Nephrology 2021;41:296–306. https://doi.org/10.1016/j.semnephrol.2021.06.002.

[5] D'Agati VD, Chagnac A, de Vries APJ, Levi M, Porrini E, Herman-Edelstein M, et al. Obesity-related glomerulopathy: clinical and pathologic characteristics and pathogenesis. Nat Rev Nephrol 2016;12:453–71. https://doi.org/10.1038/nrneph.2016.75.

[6] Praga M, Hernández E, Morales E, Campos AP, Valero MA, Martínez MA, et al. Clinical features and long-term outcome of obesity-associated focal segmental glomerulosclerosis. Nephrol Dial Transplant 2001;16:1790–8. https://doi.org/10.1093/ndt/16.9.1790.

[7] Kambham N, Markowitz GS, Valeri AM, Lin J, D'Agati VD. Obesity-related glomerulopathy: an emerging epidemic. Kidney Int 2001;59:1498–509. https://doi.org/10.1046/j.1523-1755.2001.0590041498.x.

[8] Tsuboi N, Koike K, Hirano K, Utsunomiya Y, Kawamura T, Hosoya T. Clinical features and long-term renal outcomes of Japanese patients with obesity-related glomerulopathy. Clin Exp Nephrol 2013;17:379–85. https://doi.org/10.1007/s10157-012-0719-y.

[9] Vogel L. Time to rethink refusing kidney transplants for obese patients. CMAJ 2013;185:E603. https://doi.org/10.1503/cmaj.109-4557.

[10] Lassalle M, Fezeu LK, Couchoud C, Hannedouche T, Massy ZA, Czernichow S. Obesity and access to kidney transplantation in patients starting dialysis: A prospective cohort study. PLoS One 2017;12:e0176616. https://doi.org/10.1371/journal.pone.0176616.

[11] Di Cocco P, Bencini G, Spaggiari M, Petrochenkov E, Akshelyan S, Fratti A, et al. Obesity and Kidney Transplantation-How to Evaluate, What to Do, and Outcomes. Transplantation 2023;107:1903–9. https://doi.org/10.1097/TP.0000000000004564.

[12] Jittirat A, Levea S-L, Concepcion BP, Shawar SH. Kidney Transplant and Cardiovascular-Kidney-Metabolic Health. Cardiol Clin 2025;43:441–55. https://doi.org/10.1016/j.ccl.2024.12.004.

[13] Fernando S, Varma J, Dengu F, Menon V, Malik S, O'Callaghan J. Bariatric surgery improves access to renal transplantation and is safe in renal failure as well as after transplantation: A systematic review and meta-analysis. Transplantation Reviews 2023;37:100777. https://doi.org/10.1016/j.trre.2023.100777.

[14] Timsit M-O, Aron-Wisnewsky J, Bessede T, Kassab D, Amrouche L, Bento L, et al. Kidney transplantation in adult candidates with obesity: Guidelines by the Association

Française d'Urologie and Société Francophone de Transplantation. Fr J Urol 2026;36:103100. https://doi.org/10.1016/j.fjurol.2026.103100.
[15] Chadban SJ, Ahn C, Axelrod DA, Foster BJ, Kasiske BL, Kher V, et al. KDIGO Clinical Practice Guideline on the Evaluation and Management of Candidates for Kidney Transplantation. Transplantation 2020;104:S11–S103. https://doi.org/10.1097/TP.0000000000003136.
[16] Oniscu GC, Abramowicz D, Bolignano D, Gandolfini I, Hellemans R, Maggiore U, et al. Management of obesity in kidney transplant candidates and recipients: A clinical practice guideline by the DESCARTES Working Group of ERA. Nephrol Dial Transplant 2022;37:i1–i15. https://doi.org/10.1093/ndt/gfab310.
[17] Eisenberg D, Shikora SA, Aarts E, Aminian A, Angrisani L, Cohen RV, et al. 2022 American Society of Metabolic and Bariatric Surgery (ASMBS) and International Federation for the Surgery of Obesity and Metabolic Disorders (IFSO): Indications for Metabolic and Bariatric Surgery. Obes Surg 2022;32:3019–3025. https://doi.org/10.1007/s11695-022-06332-1.
[18] Pinar U, Mageau A, Renard Y, Rod X, Lebacle C, Barrou B, et al. Pre-transplant morphometry by computed tomography scan and post-transplant dialysis risk in overweight or obese kidney transplant recipients. Int Urol Nephrol 2021;53:2469–75. https://doi.org/10.1007/s11255-021-02995-4.
[19] McPherson KC, Shields CA, Poudel B, Fizer B, Pennington A, Szabo-Johnson A, et al. Impact of obesity as an independent risk factor for the development of renal injury: implications from rat models of obesity. Am J Physiol Renal Physiol 2019;316:F316–27. https://doi.org/10.1152/ajprenal.00162.2018.
[20] Faleiros CM, Francescato HDC, Papoti M, Chaves L, Silva CGA, Costa RS, et al. Effects of previous physical training on adriamycin nephropathy and its relationship with endothelial lesions and angiogenesis in the renal cortex. Life Sciences 2017;169:43–51. https://doi.org/10.1016/j.lfs.2016.11.014.
[21] Lee VW, Harris DC. Adriamycin nephropathy: A model of focal segmental glomerulosclerosis. Nephrology 2011;16:30–8. https://doi.org/10.1111/j.1440-1797.2010.01383.x.
[22] Baroni EA, Costa RS, Volpini R, Coimbra TM. Sodium bicarbonate treatment reduces renal injury, renal production of transforming growth factor-beta, and urinary transforming growth factor-beta excretion in rats with doxorubicin-induced nephropathy. Am J Kidney Dis 1999;34:328–37. https://doi.org/10.1016/s0272-6386(99)70363-x.
[23] Sun YBY, Qu X, Zhang X, Caruana G, Bertram JF, Li J. Glomerular Endothelial Cell Injury and Damage Precedes That of Podocytes in Adriamycin-Induced Nephropathy. PLOS ONE 2013;8:e55027. https://doi.org/10.1371/journal.pone.0055027.
[24] Cheng H, Fan X, Guan Y, Moeckel GW, Zent R, Harris RC. Distinct Roles for Basal and Induced COX-2 in Podocyte Injury. J Am Soc Nephrol 2009;20:1953–62. https://doi.org/10.1681/ASN.2009010039.
[25] Mandelbaum A, Podjarny E, Bernheim J, Green J, Rathaus M. Role of thromboxane in the altered vascular reactivity of pregnant rats with adriamycin nephropathy. Nephrol Dial Transplant 1999;14:1124–8. https://doi.org/10.1093/ndt/14.5.1124.
[26] Deelman LE, Navis G, de Boer E, Wietses M, de Zeeuw D, Henning RH. Role of proteinuria in the regulation of renal renin-angiotensin system components in unilateral proteinuric rats. J Renin Angiotensin Aldosterone Syst 2003;4:38–42. https://doi.org/10.3317/jraas.2003.006.
[27] Ahmadi AR, Qi L, Iwasaki K, Wang W, Wesson RN, Cameron AM, et al. Orthotopic Rat Kidney Transplantation: A Novel and Simplified Surgical Approach. J Vis Exp 2019. https://doi.org/10.3791/59403.

[28] Arapis K, Cavin JB, Gillard L, Cluzeaud F, Lettéron P, Ducroc R, et al. Remodeling of the Residual Gastric Mucosa after Roux-En-Y Gastric Bypass or Vertical Sleeve Gastrectomy in Diet-Induced Obese Rats. PLOS ONE 2015;10:e0121414. https://doi.org/10.1371/journal.pone.0121414.
[29] Pellicer-Valero ÓJ, Massaro GA, Casanova AG, Paniagua-Sancho M, Fuentes-Calvo I, Harvat M, et al. Neural Network-Based Calculator for Rat Glomerular Filtration Rate. Biomedicines 2022;10. https://doi.org/10.3390/biomedicines10030610.
[30] Racusen LC, Solez K, Colvin RB, Bonsib SM, Castro MC, Cavallo T, et al. The Banff 97 working classification of renal allograft pathology. Kidney International 1999;55:713–23. https://doi.org/10.1046/j.1523-1755.1999.00299.x.
[31] Cavin J-B, Couvelard A, Lebtahi R, Ducroc R, Arapis K, Voitellier E, et al. Differences in Alimentary Glucose Absorption and Intestinal Disposal of Blood Glucose After Roux-en-Y Gastric Bypass vs Sleeve Gastrectomy. Gastroenterology 2016;150:454-464.e9. https://doi.org/10.1053/j.gastro.2015.10.009.
[32] Chueakula N, Jaikumkao K, Arjinajarn P, Pongchaidecha A, Chatsudthipong V, Chattipakorn N, et al. Diacerein alleviates kidney injury through attenuating inflammation and oxidative stress in obese insulin-resistant rats. Free Radic Biol Med 2018;115:146–55. https://doi.org/10.1016/j.freeradbiomed.2017.11.021.
[33] Stemmer K, Perez-Tilve D, Ananthakrishnan G, Bort A, Seeley RJ, Tschöp MH, et al. High-fat-diet-induced obesity causes an inflammatory and tumor-promoting microenvironment in the rat kidney. Dis Model Mech 2012;5:627–35. https://doi.org/10.1242/dmm.009407.
[34] López-Martínez M, Rodríguez-Martínez P, Blay L, Armengol P, Pey I, Ferrer M, et al. Bariatric Surgery Reverses ORG and Exhibits a Distinct Transcriptomic Profile Compared to Weight Loss Through a Low-Fat Diet. Int J Mol Sci 2026;27:839. https://doi.org/10.3390/ijms27020839.
[35] Adepoju L, Danos D, Green C, Cook MW, Schauer PR, Albaugh VL. Effect of high-risk factors on postoperative major adverse cardiovascular and cerebrovascular events trends following bariatric surgery in the United States from 2012 to 2019. Surg Obes Relat Dis 2023;19:59–67. https://doi.org/10.1016/j.soard.2022.08.014.
[36] Valle P, Chammas M. Microsurgical Skills: A Handbook of Experimental Microsurgical Techniques. Tercero en discordia; 2021.
[37] Hölzen JP, Palmes D, Langer M, Spiegel HU. Microsurgical training curriculum for learning kidney and liver transplantation in the rat. Microsurgery 2005;25:614–23. https://doi.org/10.1002/micr.20174.
[38] Kramer HJ, Saranathan A, Luke A, Durazo-Arvizu RA, Guichan C, Hou S, et al. Increasing body mass index and obesity in the incident ESRD population. J Am Soc Nephrol 2006;17:1453–9. https://doi.org/10.1681/ASN.2005111241.

Figure 1 : Flow of animals through the study (Series 2), presented as a CONSORT-style flow diagram adapted for a non-randomized, exploratory design. Allocation to dose and surgical subgroups was sequential and non-randomized; no randomization step is therefore shown. For each subgroup, the numbers of animals allocated, excluded (with reasons), and analysed are reported.

Figure 2 : Surgical procedures across Series

A : Sequence showing antegrade catheterization of the common jugular vein, followed by the normal appearance of a rat kidney in the context of obesity, and then the renal fatty appearance two weeks after adriamycin injection.

B : Sequence showing resection of the forestomach, followed by the construction of a sleeve gastrectomy (upper panel) or a Roux-en-Y gastric bypass (lower panel). Radiopaque contrast studies illustrate the surgical configurations.

C : Intraoperative view of kidney graft. Left panel: venous anastomosis (blue arrow), arterial anastomosis (red arrow), and ureterovesical anastomosis (black arrow). Right panel: left-sided graft in the context of ORG-ESRD. The vascular anastomoses are covered with an omental flap, the ureter is marked in violet, and the native right kidney retains its fatty appearance.

Figure 3 : Series 2 analysis

Data are shown as median (line) with range (whiskers). Measurements at each time point were obtained from partially overlapping cohorts across experimental series (not necessarily repeated measures in the same animals); therefore, curves represent cross-sectional group summaries and sample sizes vary across time points. The number of animals analysed per group is detailed in Figure 1 and the Statistical Analyses section.

A : Body weight changes in ORG-ESRD

B: Changes in creatinine clearance in ORG-ESRD

C, D, E : Development of nephrotic syndrome in ORG-ESRD

F : Development of FSGS in ORG-ESRD

Figure 4 : Bariatric effect analysis in ORG-ESRD

Data are shown as median (line) with range (whiskers). Measurements at each time point were obtained from partially overlapping cohorts across experimental series (not necessarily repeated measures in the same animals); therefore, curves represent cross-sectional group summaries and sample sizes vary across time points. The number of animals analysed per group is detailed in Figure 1 and the Statistical Analyses section.

A : Body weight changes in ORG-ESRD

B: Changes in creatinine clearance in ORG-ESRD

C, D, E : Development of nephrotic syndrome in ORG-ESRD

F : Development of FSGS in ORG-ESRD

Supplementary material :

Supplementary material 1 : Operative and Postoperative Monitoring of Invasive Procedure

Supplementary material 2 : Development of End-stage renal disease in lean rats

Supplementary material 3:

3.1 Histological scoring of renal injury in the ORG-ESRD bariatric series. Each point represents one animal; horizontal bars indicate medians and the number of animals (n) is shown per group. Semi-quantitative score (0–3): 0 = absent/normal; 1 = mild (<25%); 2 = moderate (25–50%); 3 = severe (>50% of the assessed area). Representative photomicrographs of the corresponding lesions are also shown.

3.2 Tubulointerstitial lesions (Masson's trichrome, ×200): (A) non-atrophic tubules without interstitial fibrosis or inflammation; (B) interstitial fibrosis; (C) acute tubular necrosis; (D) interstitial inflammation; (E) classic-type and (F) thyroidization-type tubular atrophy.

3.3 Focal segmental glomerulosclerosis (FSGS) of increasing severity (HES and periodic acid–Schiff, ×400): (A) without lesion; (B) light; (C) mild with podocyte hypertrophy; (D) severe with major podocyte hypertrophy and hyperplasia. All slides were scored by a single pathologist blinded to group allocation.

Supplementary material 4 : Learning Curve of Microsurgical Kidney Transplantation in Rats with End-Stage Renal Disease

Supplementary video :

- Video A1 : Macrodissection of the donor
- Video A2 : Microscopic dissection of both donor kidneys
- Video A3 : Clamping, washout and backtable
- Video A4 : Macroscopic and microscopic dissection of recipient
- Video A5 : Vascular anastomosis
- Video A6 : Ureterovesical anastomosis and graft fixation

Figures

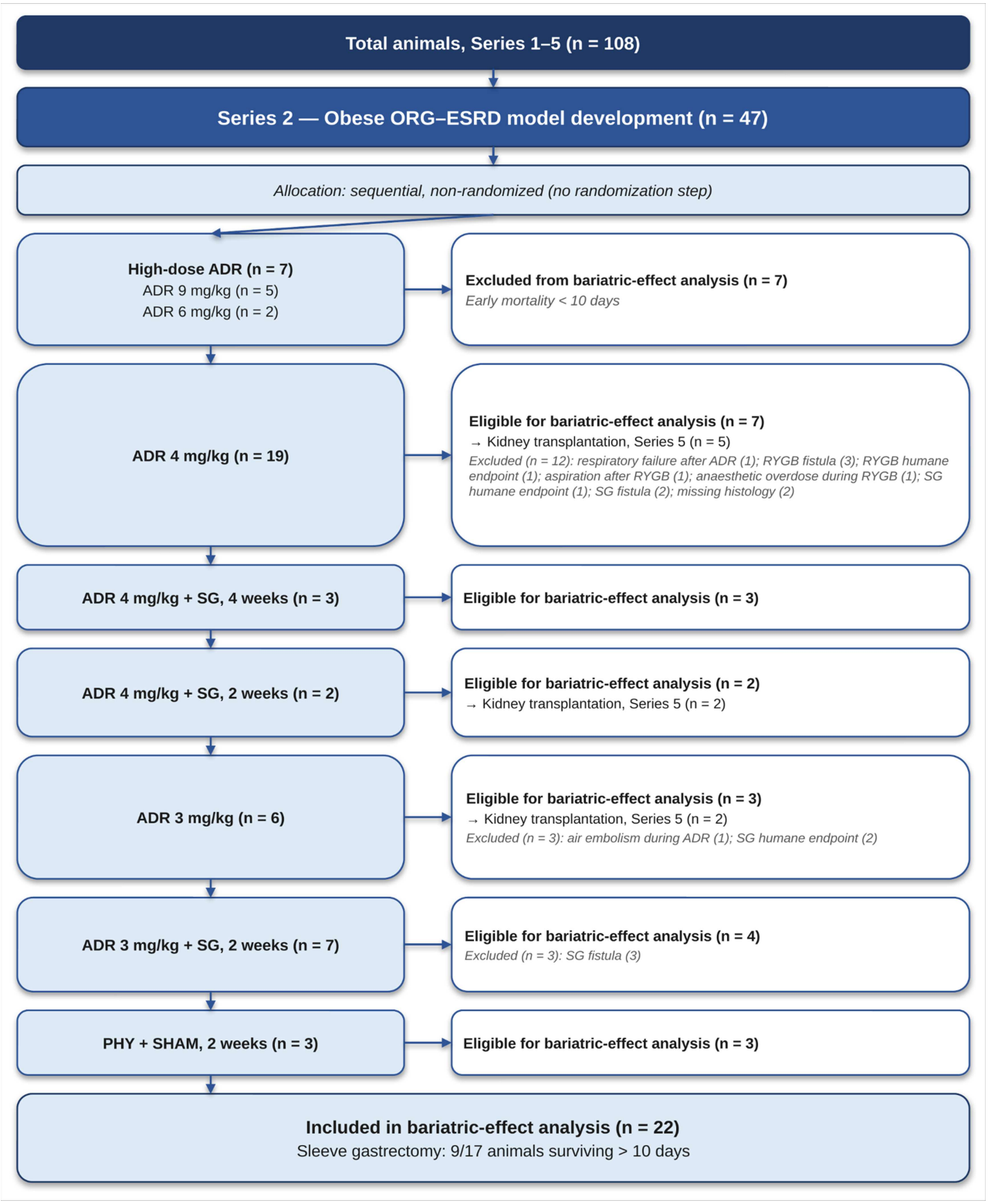


Figure 1

Flow of animals through the study (Series 2), presented as a CONSORT-style flow diagram adapted for a non-randomized, exploratory design. Allocation to dose and surgical subgroups was sequential and non-

randomized; no randomization step is therefore shown. For each subgroup, the numbers of animals allocated, excluded (with reasons), and analysed are reported.

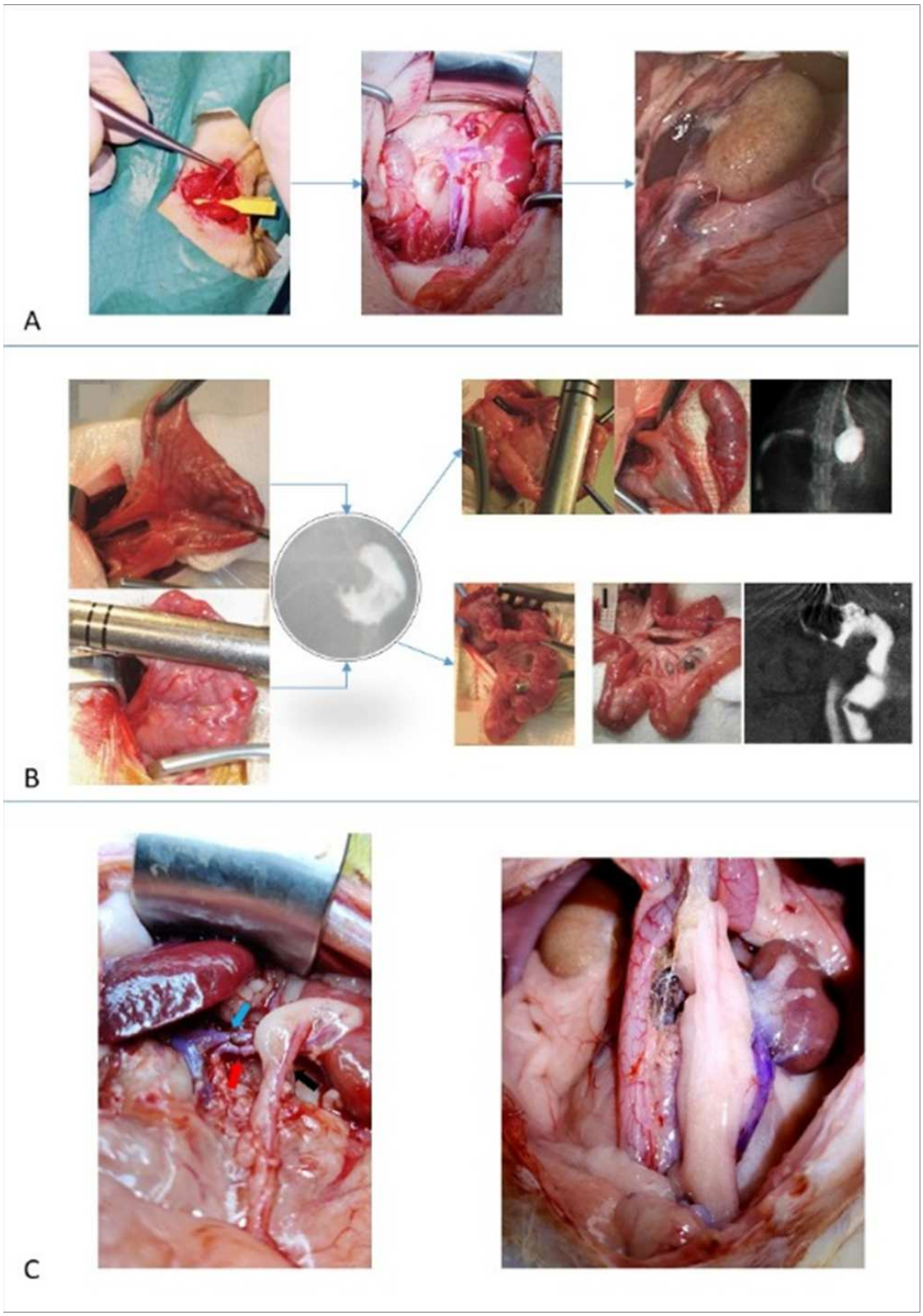


Figure 2

Surgical procedures across Series

A : Sequence showing antegrade catheterization of the common jugular vein, followed by the normal appearance of a rat kidney in the context of obesity, and then the renal fatty appearance two weeks after adriamycin injection.

B : Sequence showing resection of the forestomach, followed by the construction of a sleeve gastrectomy (upper panel) or a Roux-en-Y gastric bypass (lower panel). Radiopaque contrast studies illustrate the surgical configurations.

C : Intraoperative view of kidney graft. Left panel: venous anastomosis (blue arrow), arterial anastomosis (red arrow), and ureterovesical anastomosis (black arrow). Right panel: left-sided graft in the context of ORG-ESRD. The vascular anastomoses are covered with an omental flap, the ureter is marked in violet, and the native right kidney retains its fatty appearance.

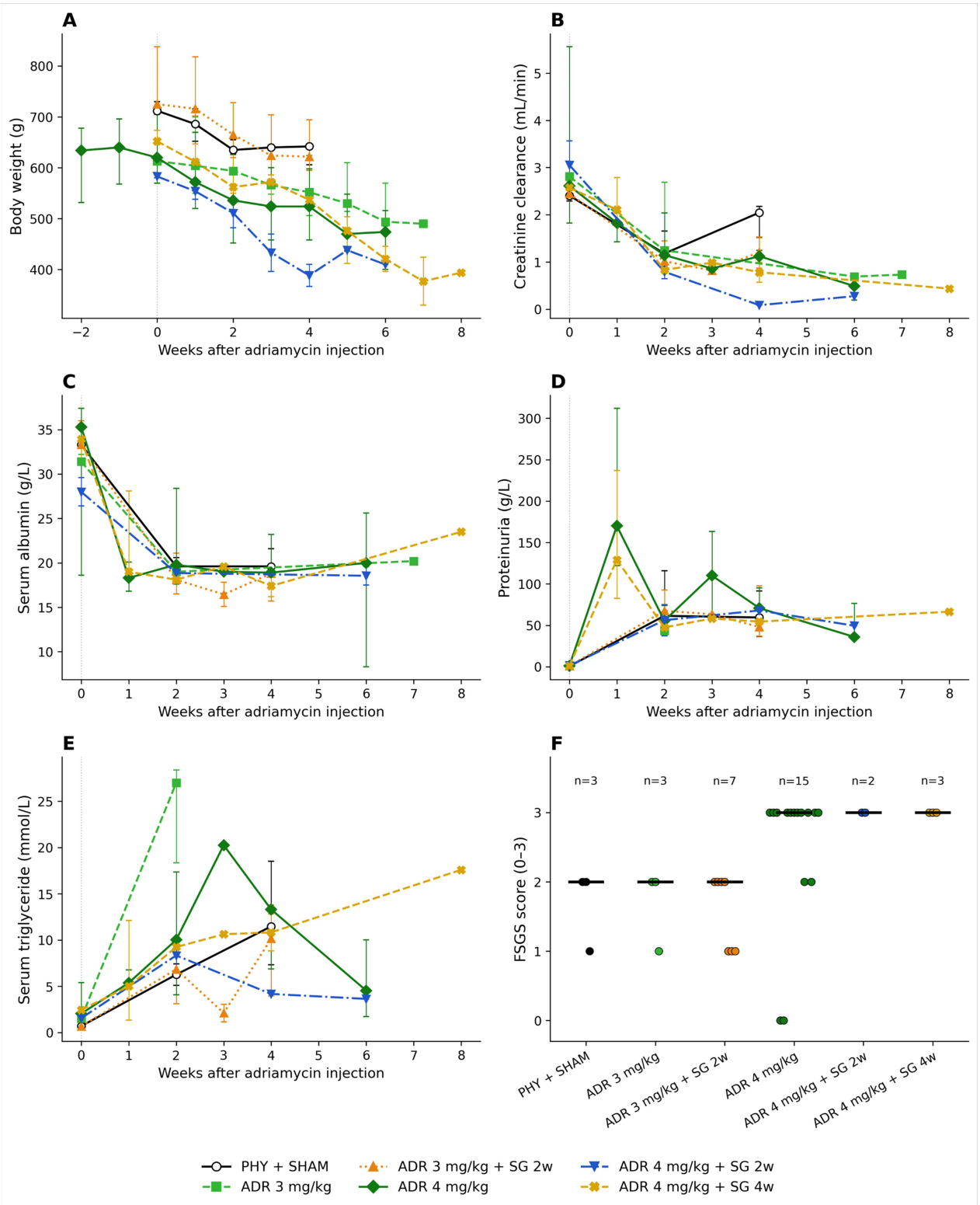


Figure 3

Series 2 analysis

Data are shown as median (line) with range (whiskers). Measurements at each time point were obtained from partially overlapping cohorts across experimental series (not necessarily repeated measures in the same animals); therefore, curves represent cross-sectional group summaries and sample sizes vary

across time points. The number of animals analysed per group is detailed in Figure 1 and the Statistical Analyses section.

A : Body weight changes in ORG-ESRD

B: Changes in creatinine clearance in ORG-ESRD

C, D, E : Development of nephrotic syndrome in ORG-ESRD

F : Development of FSGS in ORG-ESRD

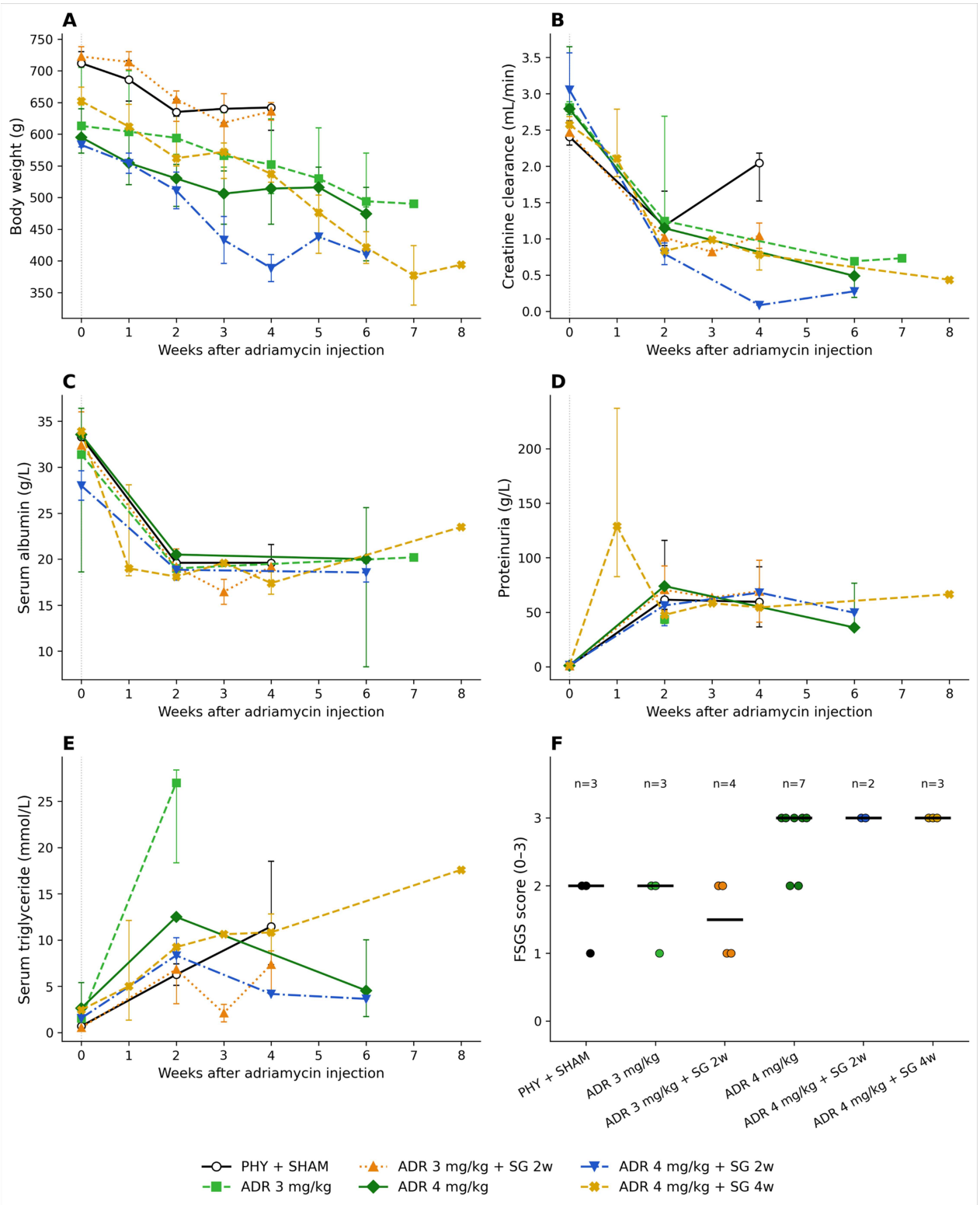


Figure 4

Bariatric effect analysis in ORG-ESRD

Data are shown as median (line) with range (whiskers). Measurements at each time point were obtained from partially overlapping cohorts across experimental series (not necessarily repeated measures in the same animals); therefore, curves represent cross-sectional group summaries and sample sizes vary

across time points. The number of animals analysed per group is detailed in Figure 1 and the Statistical Analyses section.

A : Body weight changes in ORG-ESRD

B: Changes in creatinine clearance in ORG-ESRD

C, D, E : Development of nephrotic syndrome in ORG-ESRD

F : Development of FSGS in ORG-ESRD

Supplementary Files

This is a list of supplementary files associated with this preprint. Click to download.

- Supplement1.docx
- Supplement2.docx
- Supplement3.1histologyscores.tiff
- Supplement4.docx
- Supplement3.3FSGS.tiff
- Supplement3.2tubulointerstitial.tiff
- VideoA1Macrodissectionofthedonor.mp4
- VideoA5Vascularanastomosis.mp4
- VideoA4Macroscopicandmicroscopicdissectionofrecipient.mp4
- VideoA6Ureterovesicalanastomosisandgraftfixation.mp4
- VideoA3Clampingwashoutandbacktable.mp4
- VideoA2Microscopicdissectionofbothdonorkidneyslight.mp4